Mechanical properties gradient in graphite nodules: influence on ferritic DCI damaging micromechanisms

Vittorio Di Cocco, Francesco Iacoviello, Alessandra Rossi
Università di Cassino e del Lazio Meridionale, DiCeM, via G. Di Biasio 43, 03043 Cassino (FR), Italy
v.dicocco@unicas.it

Mauro Cavallini, Stefano Natali
Università di Roma "La Sapienza", DICMA, via Eudossiana 18, Rome, Italy

Fanny Ecarla
CSM Instruments SA, Rue de la Gare 4, 2034, Peseux, Switzerland

ABSTRACT. Versatility and higher performances at lower cost if compared to these of steels with analogous performances are the main advantages of Ductile Cast Irons (DCIs).
In the last years, the research group of Metallurgy of the Università di Cassino e del Lazio Meridionale deeply investigated the damaging micromechanisms in ferritic pearlitic and austempered DCIs by means of tensile and fatigue tests, mainly performing scanning electron microscope (SEM) or Digital Microscope (DM) observations of specimens lateral surfaces during the tests ("in situ" tests).
In this work, graphite nodules mechanical behaviour is investigated by means of nano indentation tests and results are compared with the damaging micromechanisms observed in ferritic DCIs.

SOMMARIO. Le ghise sferoidali sono caratterizzate da elevate prestazioni e da una notevole versatilità. Tali caratteristiche sono disponibili ad un costo ridotto, comparando le ghise sferoidali con acciai caratterizzate da un analogo comportamento meccanico.
Negli ultimi anni, il gruppo di ricerca di Metallurgia dell'Università di Cassino e del Lazio Meridionale ha investigato in maniera approfondita i micromeccanismi di danneggiamento nelle ghise sferoidali mediante prove di trazione e prove di fatica, principalmente effettuando osservazioni delle superfici laterali durante le prove (prove "in situ") sia utilizzando un microscopio elettronico a scansione (SEM) che un microscopio digitale (DM).
In questo lavoro, il comportamento meccanico dei noduli di grafite è stato investigato mediante prove di nanodurezza ed i risultati sono stati comparati con i meccanismi di danneggiamento osservati nelle ghise sferoidali ferritiche.

KEYWORDS. Ductile cast irons; Nano indentation test; Damaging micromechanisms.

INTRODUCTION

Ductile cast irons (DCIs) are characterized by an interesting combination of good mechanical properties (similar to carbon steels) and by a good castability (peculiar of cast irons), due to the peculiar shape of the graphite elements (nodular and not lamellar). This is obtained by means a chemical compositions control adding

nodularizing elements like Mg, and not by means of long heat treatments, with a consequent strong reduction of the production costs. DCIs are widely used to produce pressure pipes and are also used in automotive industry (e.g., gears and suspensions) and for general engineering applications (e.g. in paper manufacturing industry), [1, 2].
DCIs damage micromechanisms are usually identified with voids nucleation and growth due to the matrix-graphite nodules debonding [3-9] and numerous studies provided analytical laws to describe a single void growth, depending on the void geometries and matrix behaviour. A scheme of this mechanism is summarized in Fig. 1.

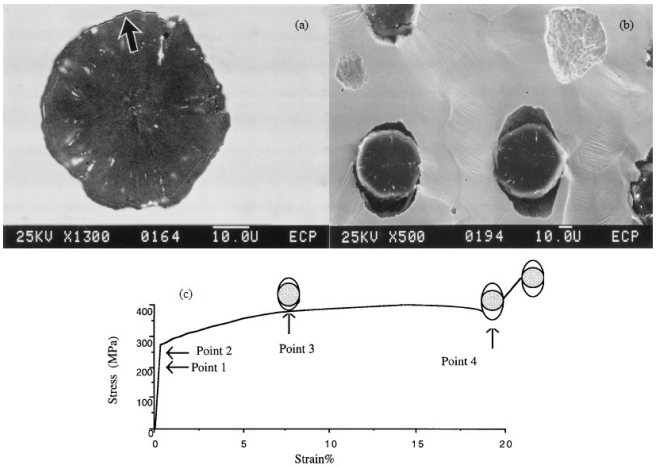

Figure 1: Matrix-graphite nodules debonding evolution during tensile test [5]. a) decohesion of the interface observed in the SEM at point 2 of the stress-strain curve; b) cavity growth around nodules (point 3 of the stress-strain curve SEM observation); c) Stress-strain curve recorded during a tensile test.

Focusing ferritic DCIs, some experimental results did not agree with the "pure" graphite nodules – ferritic matrix debonding mechanism, considering both tensile and fatigue loadings [10-13]. Focusing tensile tests [10-12], elastic stage was confirmed as characterized by a complete absence of cracks or microvoids initiations both in ferritic matrix and in graphite nodules. Corresponding to macroscopic plastic deformation stage, cracks initiated and developed in graphite elements with an "onion-like" morphology (Fig. 2). Only at very high strain values, matrix plastic deformation becomes evident, with a concurrent development of the graphite elements damage and matrix-graphite elements' debonding was only seldom observed.

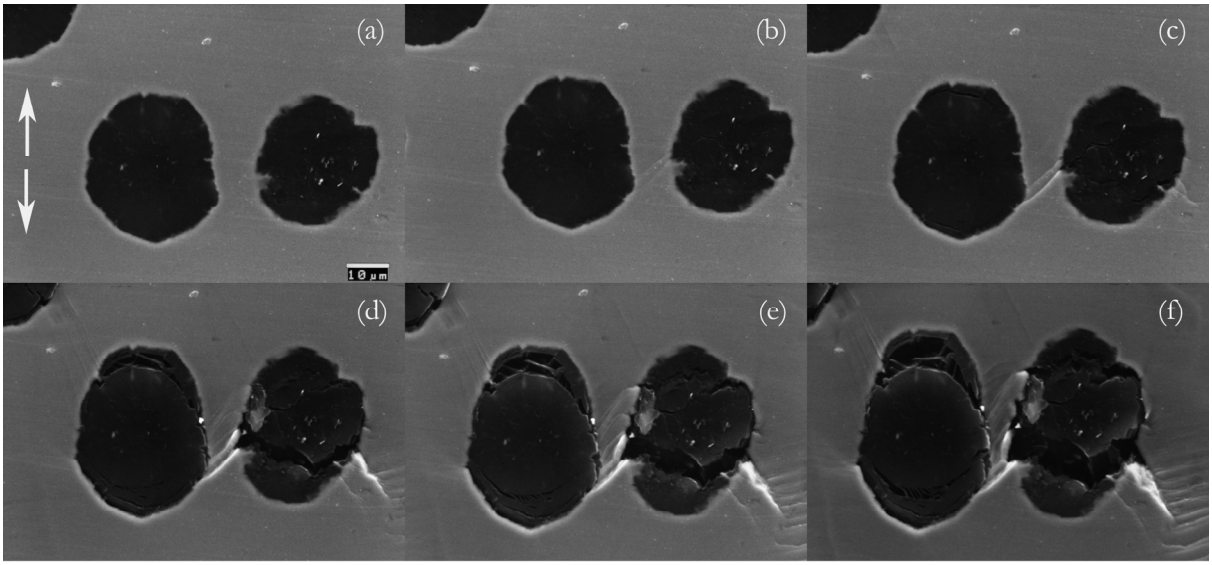

Figure 2: EN GJS400-22 ductile cast iron (strain rate of 10^{-3} s^{-1}). SEM in situ surface analysis corresponding to the following σ [MPa]–ε% values: (a) 330–2.5%, (b) 4300 – 4%, (c) 455–6%, (d) 485–10%, (e) 500–12.5% and (f) 508–16% (arrows indicate the loading direction)

Considering fatigue crack propagation [13], the authors verified that the damaging micromechanisms in graphite nodules was influenced by the loading conditions, with "pure" ferritic matrix – graphite nodules debonding that seemed to be the privileged interaction mechanism between graphite nodules and fatigue crack only for higher ΔK values. A deeper analysis of the graphite nodules seemed to be necessary.
The authors proposed a DCIs solidification and cooling process [13, 14] based on the analysis of the Fe-C-Si ternary phase diagram. According to this analysis, under the hypothesis of a cooling rate approximately equal to zero, it is possible to identify different "carbon sources" that allows an homogeneous and concentric growth of nodules on nuclei, and can be classified as follows:
- a graphite core obtained directly from the melt (C_M);
- a graphite inner shell obtained during eutectic solidifications (by means of C atoms solid diffusion through austenite shells, C_E);
- a graphite intermediate shell obtained during cooling (due to C solubility decrease in austenite, C_A);
- a graphite outer shell obtained during eutectoid transformation (due to the negligible C solubility in ferritic grains, C_F).
Graphite volume fractions obtained in the different solidification and cooling stages has been evaluated by means of a concentric homogeneous spherical growth model, and the corresponding graphite nodule radiuses R, for the investigated DCI, are:

$$\begin{aligned} R_{C_M} &= 0.26 R_{nodule} \\ R_{C_M+C_E} &= 0.90\ R_{nodule} \\ R_{C_M+C_E+C_A} &= 0.95\ R_{nodule} \end{aligned} \qquad (1)$$

Furthermore, always in [14], differences in the wear resistance between nodule core and nodule shield were qualitatively evaluated by means of traditional metallographic preparation, both considering a 3D surface reconstruction and performing a customized image processing procedures: the nodule core seemed to be characterized by a lower wearing resistance if compared to the nodule outer shield (Fig. 3).

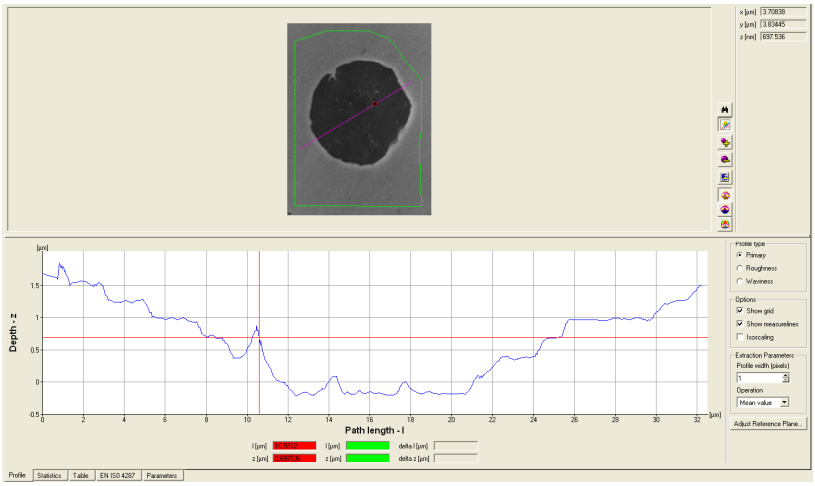

Figure 3: 3D reconstructed specimen. Profile evolution [14].

In this work the graphite nodules behaviour is analysed by means of different experimental procedures:
- EDX analysis of graphite nodules chemical composition, considering the presence of white spots inside graphite nodules (if observed by means of a SEM);
- nano indentation tests performed in different points of the graphite nodules.

MATERIAL AND EXPERIMENTAL PROCEDURES

A fully ferritic DCI with a high graphite elements nodularity (higher than 85%; 132 nodules/mm^2) has been considered (chemical composition in Tab. 1). In order to identify the presence of metallic particle inside the graphite nodules, EDX map of the graphite nodules has been performed using a Hitachi SEM, considering

metallographically prepared, but not etched, specimens.

C	Si	Mn	S	P	Cu	Cr	Mg	Sn
3.62	2.72	0.19	0.011	0.021	0.019	0.031	0.047	0.011

Table 1: Investigated fully ferritic DCI chemical composition (GJS 350-22).

Nano indentation tests have been performed by means of a CSM Nano Indentation Tester (NHT), with the following test parameters:

- ✓ Indenter type: Berkovich
- ✓ Approach speed: 2000 nm/min
- ✓ Loading type: linear
- ✓ Loading rate: 2 mN/min
- ✓ Maximum load: 1 mN
- ✓ Unloading rate: 2 mN/min

All the results were obtained using the Oliver - Pharr method (under the hypothesis of a sample Poisson's ratio of 0.3, for the elastic calculations), [15]. This method describes the upper portion of the unloading curve (Fig. 4) by a power law relationship:

$$F = F_{max}\left(\frac{h - h_p}{h_{max} - h_p}\right)^m$$

where

F: test force
F_{max}: maximum applied force
h: indentation depth under applied test force
h_p: permanent indentation depth after the removal of the test force
h_{max}: maximum indentation depth at F_{max}
m: power law constant exponent

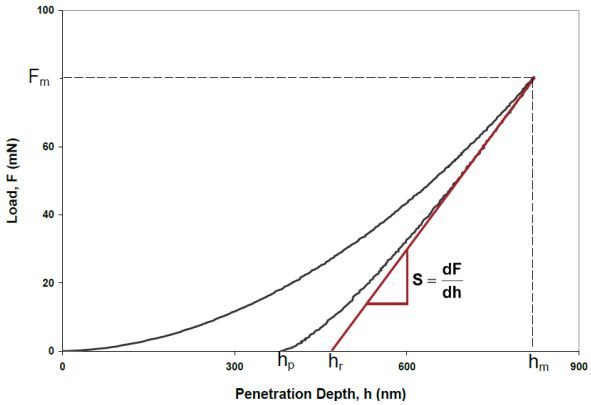

Figure 4: Typical load/displacement curve.

The contact stiffness S is given by the derivative at peak load:

$$S = \left(\frac{dF}{dh}\right)_{max} = m \cdot F_{max}\left(h_{max} - h_p\right)^{-1}$$

And the tangent depth h_r is thus given by

$$h_r = h_{max} - \frac{F_{max}}{S}$$

where h_r is the intersection of the tangent c to curve b at F_{max} with the indentation depth axis.

The contact depth (depth of the contact of the indenter with the specimen at F_{max}), h_c, is then:

$$h_c = h_{max} - \varepsilon\left(h_{max} - h_r\right)$$

The Indentation Testing Hardness H_{IT} is determined form the maximum load, F_{max}, divided by the projected contact area A_p at the contact depth h_c:

$$H_{IT} = \frac{F_{max}}{A_p \cdot h_c}$$

where

h_c: depth of the contact of the indenter with the specimen at F_{max}
A_p h_c: projected area of contact of the indenter at distance h_c from the tip
A_p: function of the contact depth (determined by a calibration of the indenter tip)
The Vickers Hardness HV is then defined as follows:

$$HV = \frac{F_{max}}{9.81 \cdot A_c \cdot h_c} \qquad (2)$$

where Ac is the developed contact area calculated form the projected contact area Ap and the indenter geometry according to the following relationship:

$$A_c = \frac{A_p}{\sin\alpha}$$

α is the angle between the axis of the diamond pyramid and its face and is equal to 68° for Vickers indenter and 65.27° for modified Berkovich indenter. Finally:

- ✓ for a Vickers indenter: $HV = 0.0945\ H_{IT}$
- ✓ for a modified Berkovich indenter: $HV = 0.0926\ H_{IT}$

It is worth to note that the mechanical properties are calculated on the assumption of a flat testing surface. If the indenter comes in to contact with a surface peak, the non-uniform contact increases the localized stress corresponding to the contact point, with a greater penetration depth and, consequently, a lower calculated hardness. In order to define the optimum testing conditions, according to International Standard ISO 14577-4, R_a value should be less than 5% of the maximum penetration depth. Anyway, nano indentation tests average values are similar on smooth or rough samples, but standard deviation value is larger in the second case (Fig. 5).

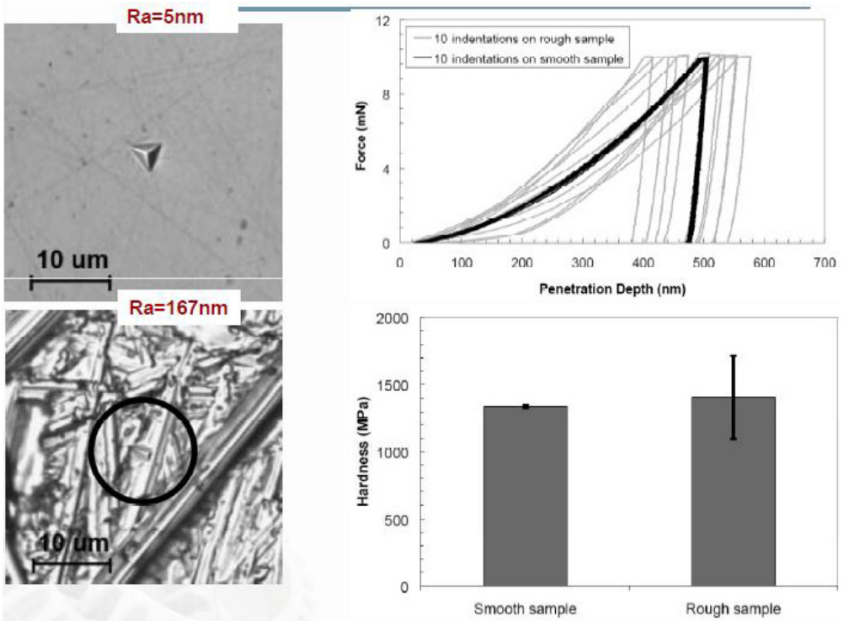

Figure 5: Specimen roughness influence on nano indentation tests results [16].

In this work, seven nodules have been considered for the nano indentation tests, following the positions in Fig. 6: nodule center, at about 1/3 R and at about 2/3 R. It is necessary to underline that the investigated sections are among the largest observed ones, hoping to perform the nano indentation tests considering equatorial sections.
Considering the discussion focused on the graphite nodule nucleation and growth described in the "Introduction" paragraph, two different results are possible:
- nano indentation tests results do not depend on the test position. Values are more or less analogous, with a dispersion that depends on the surface roughness;
- a gradient of the nano indentation tests results; in this case, considering the hypothesis of an homogenous growth of graphite nodules, a radial symmetry of the nano indentation values is expected. In this case, results should be classified according to three different groups: center, inner shield and the outer shield.

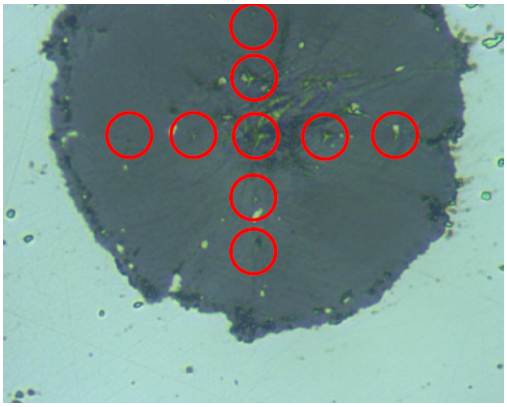

Figure 6: Graphite nodule and nano indentation test positions.

EXPERIMENTAL RESULTS AND COMMENTS

EDX map analysis

The observation of DCIs by means of a SEM often shows the presence of "white spots" inside the graphite nodules. These white spots are not randomly distributed inside the graphite nodules, but are often characterized by a sort of "radial symmetry". In this work the EDX map analysis have been performed on some nodules characterized by an unusual density of these white spots, probably due to local peculiar cooling conditions (Fig. 7).

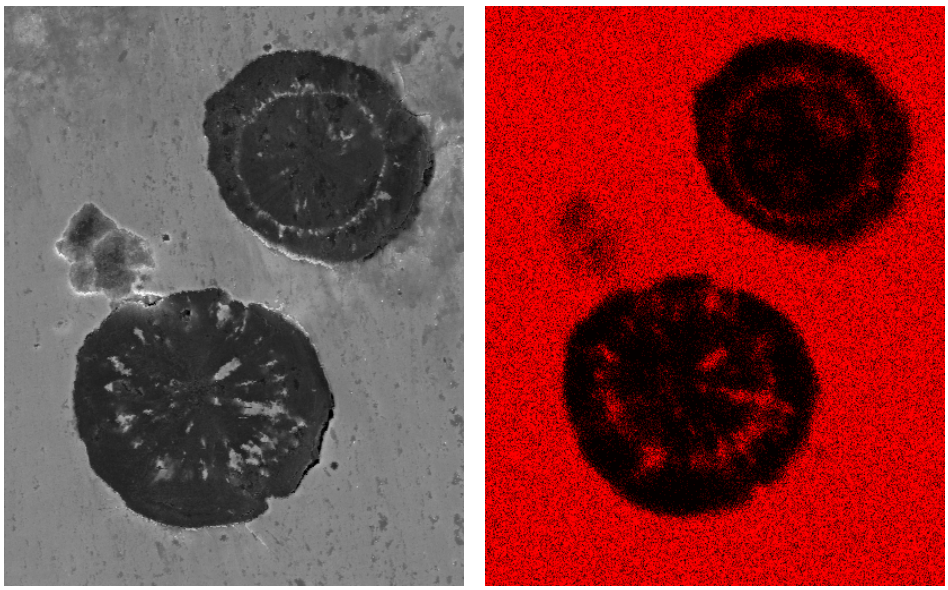

Figure 7: Graphite nodule with "white spots" (left); SEM-EDX map, Fe-K (right).

Performing an EDX map of the main alloying elements (e.g., Fig. 3b: Fe-K distribution), it is shown that these "white spots" are characterized by a chemical composition that is analogous to the ferritic matrix (considering the main alloying elements). Considering relationships (1), "white spots" are mainly distributed in the graphite inner shell obtained during eutectic solidification.

Nano indentation tests results

Considering the results of the roughness profile analysis in Fig. 3, it is evident that the graphite nodules after a metallographic preparation are not perfectly smooth: the nodule center is often characterized by a sort of plateau surrounded by a shield characterized a higher roughness. This could imply a high standard deviation of the experimental results, as already discussed in the "Material and experimental procedures" paragraph.
Although the experimental results are characterized by an important standard deviation (Fig. 8), it is evident the presence of a gradient of nano hardness values, with the lower values that are obtained in the center and the highest values that are obtained in the outer shell. This result agrees with the qualitative wearing test results [14], with the nodule cores that seemed to be characterized by a lower wearing resistance if compared to the nodule outer shield. The higher standard deviation obtained for the outer shield is due to the higher roughness values observed in this zone (Fig. 3).

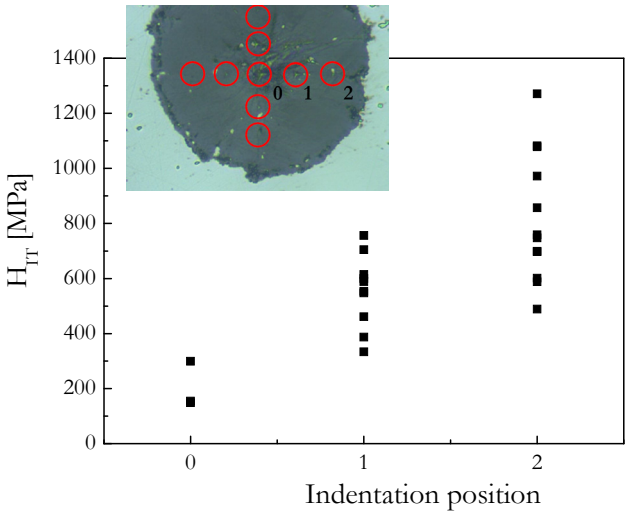

Figure 8: Nano indentations test results.

Comments

According to the experimental results, it is possible to say that the initiation and growth of graphite nodules during DCIs solidification and cooling imply a mechanical properties gradient inside the graphite nodules, with the nodule core that is characterized by a lower hardness and wear resistance if compared to the outer shell. Furthermore, during the solidification process, it is possible that metal matrix particles are embedded inside the graphite nodules, especially, but not uniquely, during the eutectic solidification, with a consequent influence on the graphite nodule mechanical behaviour (to be evaluated).
The presence of a mechanical properties gradient inside the graphite nodules can be connected to the damaging micromechanisms observed both considering tensile tests and considering fatigue crack propagation.
Considering the tensile tests, the internal damage evolution has been already described in Fig. 2. It is worth to note that the damage evolution can be considered as a sort of "ductile" mechanism, with the damage that increase only with the increase of the macroscopic applied deformation. In fact, if the test is stopped, the nodule damaging does not evolve also after 40 days with the same applied macroscopic deformation (Fig. 9, $\varepsilon\% = 8$):
- no debonding ferritic matrix – graphite nodule is observed;
- no "onion like" mechanism evolution is observed;
- no internal cracks propagation is observed;
- no new cracks initiation is observed.

This confirm that the damaging inside the graphite nodules is stable and needs an increase of the applied load (or of the applied macroscopic deformation) to increase (see Fig. 2).

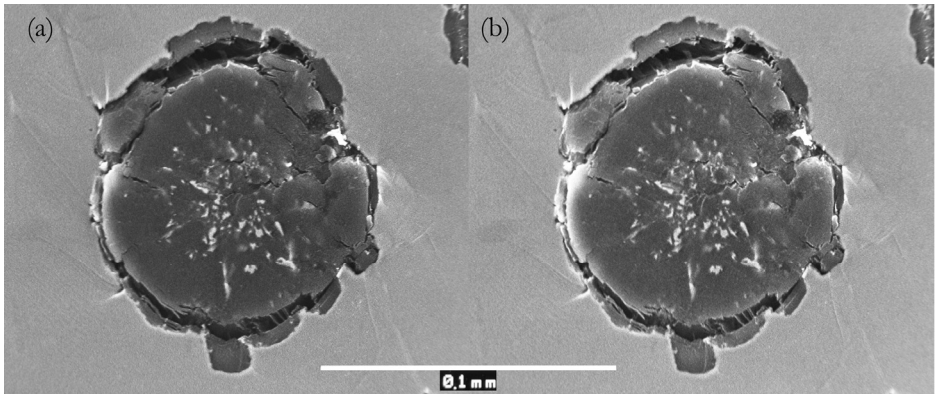

Figure 9: SEM observation of a damaged nodule with a constant value of the applied macroscopic deformation (ε% = 8). No evolution of the damage has been observed after (a) 300 s and (b) 40 days.

Considering fatigue crack propagation, the damaging mechanism is more complex due to the interaction between a main propagating crack and a substantially composite microstructure, as a ferritic DCI can be considered especially for lower ΔK and R values (stress intensity factor amplitude and stress ration, respectively). Damage inside graphite nodules seems to be dependent on the loading conditions. Corresponding to lower ΔK and R values, the ferritic DCI cannot be considered as an homogeneous material, and ferritic matrix-graphite nodules debonding is only partially developed, with graphite nodules that are characterized by an internal damage, with an evident debonding between the graphite core obtained during solidification and the graphite outer shell obtained during the cooling process (Fig. 10 and 11).

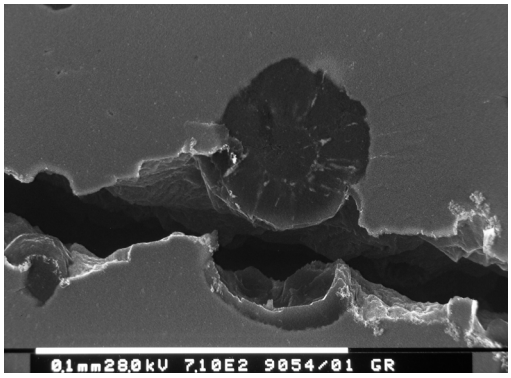

Figure 10: Ferritic DCI. SEM observation of the lateral surface of a CT (Compact Type) specimen: debonding between the graphite core obtained during solidification and the graphite outer shell obtained during the cooling process. Crack propagates from left to right.

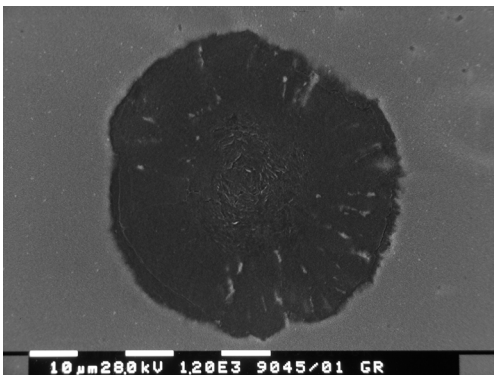

Figure 10: Ferritic DCI. SEM observation of the lateral surface of a CT (Compact Type) specimen: debonding between the graphite core obtained during solidification and the graphite outer shell obtained during the cooling process. Nodule in the crack tip plastic zone.

CONCLUSIONS

In this work the damaging micromechanisms of a ferritic DCI are analysed, considering both tensile tests and fatigue crack propagation tests, focusing the role played by the graphite nodules and the presence of a mechanical properties gradient inside the graphite nodules. According to the obtained experimental results, the following conclusions can be summarized:

- graphite nodules are characterized by an internal mechanical properties gradient, with the core (obtained directly from the melt) that is characterized by lower nano hardness values and wearing resistance and the outer shield (obtained according to carbon solid diffusion mechanism) that is characterized by higher nano hardness values and wearing resistance;
- graphite nodules show the presence of particles with a chemical composition that is analogous to the ferritic matrix;
- graphite nodule internal damage evolution is characterized by a "stable" mechanism and need an increase of the applied load (or of the applied macroscopic deformation) to evolve.

According to the authors, a deeper investigation is needed, both to improve the specimens preparation in order to decrease the nodule roughness (and, consequently, the nano indentation tests results dispersion) and to analyse the behaviour of the graphite nodules embedded in different matrix (e.g. pearlitic, ferritic-pearlitic etc.)

REFERENCES

[1] C. Labrecque, M. Gagne, Can. Metall. Quart., 37 (1998) 343.
[2] L. R. Jeckins, R. D. Forrest, Properties and selection: iron, steels and high performance alloys. ASM Handbook Ductile Iron, Metal Park (OH) ASM International, 1 (1993) 35.
[3] L. Eldoky, R.C.Voigt, AFS Trans., 86-104 (1986) 631.
[4] R. C. Voigt, L. M. Eldoky, H.S. Chiou, AFS Trans., 94 (1986) 645.
[5] M.J. Dong, C. Prioul, D. François, Metall. And Mater. Trans. A, 28A (1997) 2245.
[6] K. S. Zhang, J.B. Bai, D. François, Int. J. of Solids and Structures, 36 (1999) 3407.
[7] C. Guillermer-Neel, X. Feaugas, M. Clavel, Metall. And Mater. Trans. A, 31A (2000) 3063.
[8] C. Berdin, M.J. Dong, C. Prioul, Engineering Fracture Mechanics, 68 (2001) 1107.
[9] J. H. Liu, X.Y. Hao, G.L. Li, G.Sh.Liu, Mater. Letters, 56 (2002) 748.
[10] F. Iacoviello, V. Di Cocco, V. Piacente, O. Di Bartolomeo, Mater. Science and Engng. A, 478 (2008) 181.
[11] V. Di Cocco, F. Iacoviello, M. Cavallini, Engineering Fracture Mechanics, 77 (2010) 2016.
[12] F. Iacoviello, V. Di Cocco, M. Cavallini, Frattura ed Integrità Strutturale, 13 (2010) 3.
[13] V. Di Cocco, F. Iacoviello, A. Rossi, M. Cavallini, S. Natali, Fatigue & Fracture of Engineering Materials & Structures, (2013, in press).
[14] M. Cavallini, V. Di Cocco, F. Iacoviello, D. Iacoviello, In: Atti del XXI Convegno Nazionale del Gruppo Italiano Frattura (IGF), Cassino, Italy, (2011) 415.
[15] W.C. Oliver, G.M. Pharr, J. Mater. Res., 7 (1992) 1564.
[16] F. Ecarla, CSM Instruments Analytical Report A13b-013 (2013).